

Competition between pairing and ferromagnetic instabilities in ultracold Fermi gases near Feshbach resonances

David Pekker¹, Mehrtash Babadi¹, Rajdeep Sensarma², Nikolaj Zinner^{1,3}, Lode Pollet¹, Martin W. Zwierlein⁴, Eugene Demler¹

¹ *Physics Department, Harvard University, Cambridge, Massachusetts 02138, USA*

² *Condensed Matter Theory Center, University of Maryland, College Park, Maryland 20742, USA*

³ *Department of Physics and Astronomy, Aarhus University, Aarhus, DK-8000, Denmark*

⁴ *MIT-Harvard Center for Ultracold Atoms, Research Laboratory of Electronics, and Department of Physics, Cambridge, MA 02139, USA*

We study the quench dynamics of a two-component ultracold Fermi gas from the weak into the strong interaction regime, where the short time dynamics are governed by the exponential growth rate of unstable collective modes. We obtain an effective interaction that takes into account both Pauli blocking and the energy dependence of the scattering amplitude near a Feshbach resonance. Using this interaction we analyze the competing instabilities towards Stoner ferromagnetism and pairing.

Ferromagnetism in itinerant Fermions is a prime example of a strongly interacting system. Most theoretical treatments rely on a mean-field Stoner criterion [1], but whether this argument applies beyond mean-field remains an open problem. It is known that the existence of the Stoner instability is very sensitive to the details of band structure and interactions [2–4], however how to account for these details in realistic systems remains poorly understood. Exploring the Stoner instability with ultracold atoms has recently attracted considerable attention. Following theoretical proposals [5], the MIT group made use of the tunability [6] and slow time scales [7–10] of ultracold atom systems to study the Stoner instability [11]. Signatures compatible with ferromagnetism, as understood from mean-field theory [12], were observed in experiments: a maximum in cloud size, a minimum in kinetic energy and a maximum in atomic losses at the transition. However, no magnetic domains were resolved.

An important aspect of the MIT experiments is that they were done dynamically: the Fermi gas was originally prepared with weak interactions and then the interactions were ramped to the strongly (repulsive) regime. Dynamic rather than adiabatic preparation was used in order to avoid production of molecules. This raises the question of what are the dominant instabilities of the Fermi gas in the vicinity of a Feshbach resonance.

Naively, one would expect that on the BEC-side, molecule production is slow, as it requires a three-body process. Therefore, instability towards Stoner ferromagnetism would dominate over the instability toward molecule production. In this picture, one would expect that quenches to the attractive (BCS) regime always yield an instability towards pairing, whereas quenches to the repulsive (BEC) regime an instability towards ferromagnetism for sufficiently strong interactions.

In this Letter, we argue that this picture, which was used to interpret the MIT experiments, is incomplete. Near the Feshbach resonance, even on the BEC side, pair production remains a fast two-body process as long as the Fermi sea can absorb the molecular binding energy. As a result, near the Feshbach resonance, both on the BEC and the BCS side, the pairing and the Stoner instabilities compete directly. We now

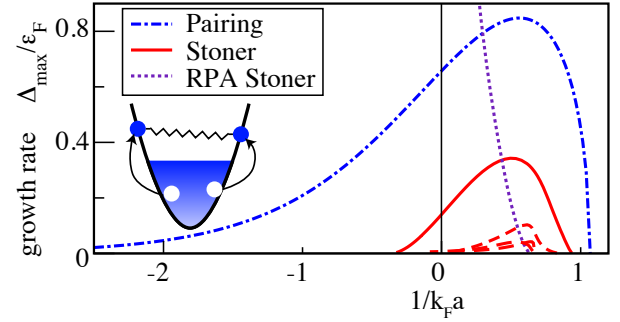


FIG. 1: Growth rate of the pairing and Stoner ferromagnetic instabilities after a quench as a function of the final interaction strength $1/k_F a$. Final interactions with negative (positive) values of $1/k_F a$ correspond to the BCS (BEC) side of the Feshbach resonance. The Stoner instability simultaneously occurs in multiple channels. The most unstable channel is indicated by the solid red line, the others by dashed red lines. The “RPA Stoner” instability corresponds to the RPA result with bare as opposed to Cooperon-mediated interaction (see text and Ref. [13]).

Inset: Schematic diagram of the pair creation process showing the binding energy (spring) being absorbed by the Fermi sea (arrows).

discuss these instabilities and their competition in detail.

We start by describing the inter-atomic interactions. A Feshbach resonance enables tunable interactions between ultracold atoms by coupling the collision partners to a molecular state with different magnetic moment. For broad resonances, where the coupling is much larger than the Fermi energy, this can be modelled by a single collision channel that supports one shallow bound state [14]. An often used, but pathological choice, is to describe repulsive interactions with a hard-sphere pseudo-potential. Instead, one should use the full T-matrix that includes the molecular bound state [15]. Although at low energies the scattering amplitude from the hard-sphere potential and the T-matrix match, at higher energies comparable to the molecular binding energy, they do not. Specifically, in the strong interaction regime where the Stoner instability is expected to occur, the Fermi energy is comparable to the binding energy of a molecule in vacuum, precluding the use of the hard-sphere potential.

In light of this remark, we study the initial dynamics of the collective modes of a Fermionic system after a sudden quench, taking the Cooperon (full T-matrix and Pauli blocking) into account. We focus on the case of a sudden quench, as it is simpler and captures the essential physics of the instability of the Fermi surface. Extensions to finite rate quenches are discussed in Ref. [13]. Our main findings are summarized in Fig. 1 and are: (1) We find that with the full T-matrix the Stoner instability survives with a finite growth rate in the range $-0.2 \lesssim k_F a \lesssim 1$, where a is the scattering length and k_F is the Fermi momentum. In contrast, using bare interactions [13] results in an unphysical divergence of the growth rate at unitarity and no magnetic instabilities on the BCS side (see Fig. 1). (2) The pairing instability persists on the BEC side, where it competes with the Stoner instability. (3) Within our approximations, the pairing instability is stronger.

At first sight, the survival of the pairing and Stoner instabilities on the wrong side of the resonance is quite remarkable. However, both can be understood by taking into account the presence of the Fermi sea. On the BEC side, due to Pauli blocking, the binding energy of the pair-like molecule can be absorbed by the two holes that are left behind (see the inset of Fig. 1). Thus, the two-body pairing process becomes forbidden when the binding energy $\sim 1/ma^2$ exceeds the maximum energy that can be absorbed by the holes $\sim k_F^2/m$ (m is the Fermion mass, a the scattering length, k_F the Fermi momentum, and throughout this Letter we use the units in which $\hbar = 1$). On the BCS side, although interactions at low energies are indeed attractive, the same is not true at high energies. As the Stoner instability involves all scattering energies up to the Fermi energy, it is natural that it can persist around unitarity, even on the BCS side.

Formalism – We consider a system of interacting Fermions described by the Hamiltonian:

$$H = \sum_{\mathbf{k}, \sigma} \xi_{\mathbf{k}\sigma} c_{\mathbf{k}\sigma}^\dagger c_{\mathbf{k}\sigma} + \int d^d \mathbf{r} U(t, \mathbf{r} - \mathbf{r}') c_{\mathbf{r}\uparrow}^\dagger c_{\mathbf{r}'\downarrow}^\dagger c_{\mathbf{r}'\downarrow} c_{\mathbf{r}\uparrow}, \quad (1)$$

where $c_\sigma^\dagger (c_\sigma)$ are the Fermion creation (annihilation) operators with spin σ , $\xi_{\mathbf{k}\sigma} = k^2/2m - \mu_\sigma$, μ_σ are the chemical potentials, and $U(t, \mathbf{r} - \mathbf{r}')$ is the time dependent pseudo-potential that describes the inter-atomic interaction. We focus on the instantaneous quench limit, in which the coupling U changes from a negligible initial value U_i to a final value U_f at time $t = 0$. In this limit, we can describe short time dynamics of a collective mode at momentum q using the corresponding susceptibility, $\chi_q(\omega_q; U_f)$, evaluated with final interactions but initial Fermionic configuration [13, 16]. In particular, if $\chi_q(\omega_q; U_f)$ has poles at $\omega_q = \Omega_q + i\Delta_q$ in the upper half of the complex plane, then fluctuations that occur after the quench will grow exponentially in time. Next, we obtain a universal description of interactions created by the pseudo-potential $U(\mathbf{r})$ by modifying the T-matrix formalism to take into account Pauli blocking, and apply these ideas to the Stoner and BCS instabilities.

Cooperon – In this section, we obtain the Cooperon, C , i.e.

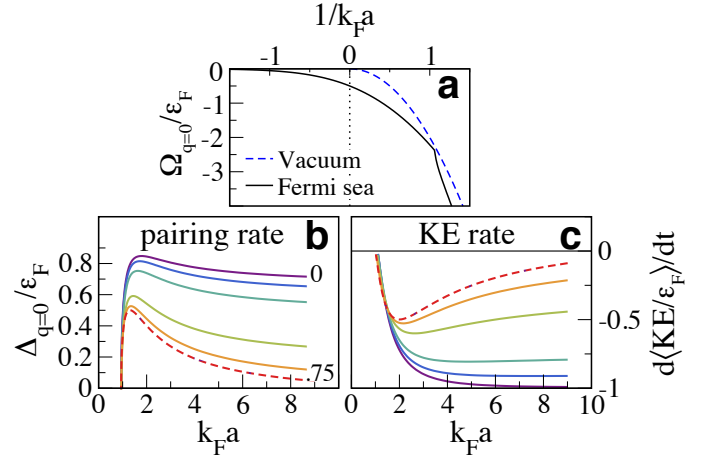


FIG. 2: Pairing instability. (a) “Binding energy” of a Feshbach molecule in vacuum and in the presence of a Fermi sea (relative to $2\epsilon_F$) as a function of interaction strength, corresponding to the real part of the T-matrix pole frequency $\Omega_{q=0} = \text{Re}[\omega_{q=0}]$. Pauli blocking by the Fermi sea results in stronger binding across the resonance. The kink occurs when the pair becomes stable. (b) Pairing rate and (c) rate of change of Kinetic Energy as a function of interaction strength on the BEC side for various temperatures [$T = 0$ (purple, solid), 0.12, 0.22, 0.5, 0.66, 0.75 T_F (red, dashed)]. Temperature is more effective at suppressing pair production at larger values of $k_F a$ as the binding energy is smaller, thus the peaks in (b) and (c) become sharper at higher temperatures. The peaks in growth rate and kinetic energy rate qualitatively match experiments [11]. Sharp onset at $k_F a \approx 1.1$ is expected to be smoothed by three-body processes.

the T-matrix that takes into account Pauli blocking of states by the Fermi sea (see Fig. 3), which is needed for an accurate study of instabilities near a Feshbach resonance.

In the center of mass frame in vacuum, the scattering of a pair of particles with identical masses m near a wide Feshbach resonance is described by the T-matrix (scattering amplitude)

$$\tau(E) = \frac{m}{4\pi} \left(\frac{1}{a} + i\sqrt{mE} \right)^{-1}. \quad (2)$$

Here, E is the energy of the scattered particles and the pseudo-potential $U(\mathbf{r} - \mathbf{r}')$ that appears in Eq. 1 is related to the T-matrix via the Lippmann-Schwinger equation. To correctly renormalize the Cooperon, we compare the Lippmann-Schwinger equations in a Fermi sea and in vacuum. For the Cooperon we can not just use the center of mass frame, as the Fermi sea breaks translational invariance. Therefore, we use the laboratory frame for both to obtain

$$C^{-1}(E, \mathbf{q}) = \tau^{-1}(E + 2\epsilon_f - \mathbf{q}^2/4m) + \int \frac{d^3 \mathbf{k}}{(2\pi)^3} \frac{n^F(\frac{\mathbf{q}}{2} + \mathbf{k}) + n^F(\frac{\mathbf{q}}{2} - \mathbf{k})}{E - \epsilon_{\frac{\mathbf{q}}{2} + \mathbf{k}} - \epsilon_{\frac{\mathbf{q}}{2} - \mathbf{k}}}. \quad (3)$$

Here, E and \mathbf{q} are the center of mass frequency and momentum of the pair, ϵ_f is the Fermi energy, $n^F(\mathbf{k})$ is the Fermi function, and $\epsilon_{\mathbf{k}} = \mathbf{k}^2/2m - \epsilon_f$. Our approach is analogous

to the one used for the Fermi-polaron problem [17].

Pairing instability – The Cooperon enters the pairing susceptibility via

$$\chi_{\text{pair}}(\vec{q}) = \int d\vec{k}_1 d\vec{k}_2 G(\vec{k}_1) G(\vec{q} - \vec{k}_1) C(\vec{q}) \times G(\vec{k}_2) G(\vec{q} - \vec{k}_2), \quad (4)$$

where \vec{q} stands for the external frequency and momentum vector $\{E, \mathbf{q}\}$, $d\vec{k}_1$ stands for $d\omega_1 d\mathbf{k}_1 / (2\pi)^4$, and $G(\vec{k}_1) = G(\omega_1, \mathbf{k}_1)$ is the bare Fermionic Green function in the non-interacting Fermi sea corresponding to the initial state. The poles of the pairing susceptibility correspond thus to the poles of the Cooperon, whose structure we now explain.

We begin our analysis with the T-matrix in vacuum. For each value of the scattering length, the T-matrix has a line of poles on the BEC side located at $\omega_q = \Omega_q + i\Delta_q = -1/ma^2 + mq^2/4$, corresponding to the binding energy of a Feshbach molecule with center of mass momentum q . As a consequence of energy and momentum conservation the pole frequency is strictly real ($\Delta_q = 0$), indicating that a two-body process in vacuum cannot produce a Feshbach molecule.

In the presence of a Fermi sea, the states below the Fermi surface are Pauli-blocked, shifting the poles of the Cooperon relative to the T-matrix in vacuum in two important ways. First, the real part of the pole Ω_q , which would correspond to the binding energy of a pair in the absence of an imaginary part, uniformly shifts down (see Fig. 2a). This shift is a result of Pauli blocking [18], and indicates an appearance of a paired state on the BCS side as well as stronger binding of the pair on the BEC side. Second, in the range $-\infty < 1/k_F a \lesssim 1.1$ the pole acquires a positive imaginary part Δ_q that corresponds to the growth rate of the pairing instability. As depicted in Fig. 1, the growth rate of the pairing instability increases exponentially $\Delta_{q=0} \approx 8\epsilon_F e^{\pi/2k_F a - 2}$ as one approaches the Feshbach resonance from the BCS side, *i.e.* the growth rate of the BCS pairing is equal to the BCS gap at equilibrium [18]. On the BEC side, the growth rate continues to increase, reaching a maximum at $k_F a \approx 2$, and finally decreasing to zero at $k_F a \approx 1.1$, at which point the Fermi sea can no longer absorb the energy of the Feshbach molecule in a two-body process. Pairing deeper in the BEC regime takes place via the more conventional three-body process and would round the pairing instability curve near $k_F a \approx 1.1$ in Fig. 1.

So far, we have concentrated on the instability at $q = 0$. We find that $q = 0$ is indeed the most unstable wavevector throughout the Feshbach resonance, but the growth rate remains finite up to $q = q_{\text{cut}}$. Throughout the resonance the approximation $q_{\text{cut}} \approx (\sqrt{3}/2)(\Delta_{q=0}/\epsilon_F)k_F$ works reasonably well except in the vicinity of $k_F a \sim 2$ where q_{cut} reaches the maximal value for a two-body process of $2k_f$.

Stoner instability – One can expect that a rapid quench to the BEC side of the resonance, where interactions are strongly repulsive, results in an instability towards Stoner ferromagnetism. We shall assume that right after the quench, the atoms are still in the free Fermi sea initial state and the Stoner insta-

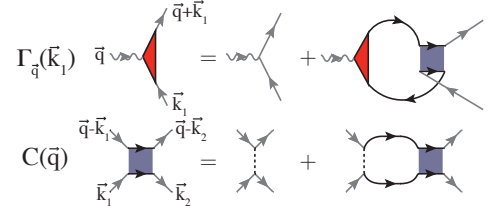


FIG. 3: Diagrams for the vertex function Γ and Cooperon C . Solid lines represent bare fermion propagators, dashed lines interactions, and wavy lines external sources. External legs, represented by gray lines, are shown for clarity.

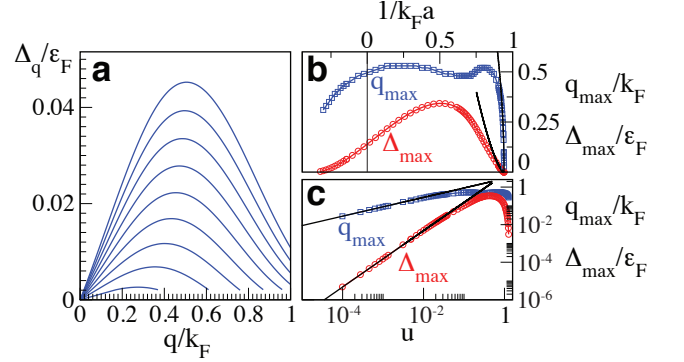


FIG. 4: Properties of growing collective modes in the Stoner instability in 3D. (a) Growth rate of the most unstable mode Δ_q as a function of wavevector q for $T = 0$ and $1/k_F a = 0.85$ (top line), 0.86, 0.87, ..., 0.93 (bottom line). (b) The most unstable wavevector q_{max} (blue) and the corresponding growth rate Δ_{max} (red) vs. $1/k_F a$. A fit to the mean-field critical theory ($\nu = 1/2$, $z = 3$) is shown with black lines [19]. (c) Details of the critical behavior of q_{max} and Δ_{max} as a function of distance from the transition point $u = (1/k_F a)_c - (1/k_F a)$, $(1/k_F a)_c \approx 0.94$.

bility is competing with the pairing instability. Our goal is to compute the ferromagnetic susceptibility using the Cooperon to describe effective inter-atomic interactions. Using the full Cooperon allows us to include three important aspects of the problem: energy dependence of the scattering amplitude near the Feshbach resonance; Pauli blocking, which renormalizes the energy of the virtual two particle bound states involved in scattering; and Kanamori-like many-body screening [4].

Technically, we compute the vertex function $\Gamma_{\omega, \mathbf{q}}(\omega_1, \mathbf{k}_1)$, which is related to the susceptibility via

$$\chi_{\text{FM}}(\vec{q}) = \int d\vec{k}_1 G(\vec{q} + \vec{k}_1) G(\vec{k}_1) \Gamma_{\vec{q}}(\vec{k}_1). \quad (5)$$

We note, that the poles of the susceptibility and the vertex function coincide. Replacing the point contact interaction vertex by the Cooperon in an RPA type resummation of the vertex function (see Fig. 3 and Ref. [4]) we obtain

$$\Gamma_{\vec{q}}(\vec{k}_1) = 1 + \int d\vec{k}_2 \Gamma_{\vec{q}}(\vec{k}_2) C(\vec{k}_1 + \vec{k}_2 + \vec{q}) G(\vec{k}_2 + \vec{q}) G(\vec{k}_2). \quad (6)$$

To compute the vertex function, a number of approximations are unavoidable. First, we assume that \mathbf{q} and ω are both small, which is valid in the vicinity of the Stoner transition. Second, in the spirit of Fermi liquid theory, we assume that the most important poles come from the Green functions, and thus we replace $G(\mathbf{k}_2 + \mathbf{q}, \omega_2 + \omega)G(\mathbf{k}_2, \omega) \rightarrow \frac{2\pi}{v_F} \frac{\mathbf{q} \cdot \mathbf{k}_2}{m \omega - \mathbf{q} \cdot \mathbf{k}_2} \delta(\omega) \delta(|\mathbf{k}_2| - k_F)$ [18]. We then obtain

$$\Gamma_{\mathbf{q}, \omega}(\hat{\mathbf{k}}_1) = 1 + \int \frac{d\hat{\mathbf{k}}_2}{4\pi} \Gamma_{\mathbf{q}, \omega}(\hat{\mathbf{k}}_2) C(\hat{\mathbf{k}}_1 + \hat{\mathbf{k}}_2, \omega) I_{\mathbf{q}, \omega}(\hat{\mathbf{k}}_2), \quad (7)$$

where

$$I_{\mathbf{q}, \omega}(\hat{\mathbf{k}}_2) = \int \frac{k_2^2 dk_2}{2\pi^2} \frac{n_F(\mathbf{k}_2 - \mathbf{q}/2) - n_F(\mathbf{k}_2 + \mathbf{q}/2)}{\omega - \epsilon_{\mathbf{k}_2 - \mathbf{q}/2} + \epsilon_{\mathbf{k}_2 + \mathbf{q}/2}}, \quad (8)$$

and $\hat{\mathbf{k}}$ indicates a vector on the Fermi surface. We thus make the approximation that we can replace \mathbf{k}_1 and \mathbf{k}_2 by $\hat{\mathbf{k}}_1$ and $\hat{\mathbf{k}}_2$ when we evaluate the value of the Cooperon. In other words, we assume that the Cooperon changes slowly compared to the Green functions. The approximation is fully justified for weak interactions, where the Cooperon is momentum and frequency independent, and the vertex function matches the RPA result [13]. For strong interactions, the Stoner instability is not driven by the pole of the Cooperon, and we therefore believe that our approximation captures the essential physics.

In the range $-0.2 \lesssim 1/k_F a \lesssim 1.0$, there is one or more lines of complex poles with a positive imaginary part $\Delta_{\mathbf{q}}$, which corresponds to the Stoner instability in different channels (a combination of momentum and orbital moment). As $q \rightarrow 0$, the different instabilities can be identified as different angular momentum channels. Since magnetization is a conserved order parameter, in each channel $\Delta_{\mathbf{q}}$ grows linearly for small q . At large q the cost of bending the order parameter results in the vanishing of $\Delta_{\mathbf{q}}$ for $q > q_{\text{cut}}$. In between, $\Delta_{\mathbf{q}}$ reaches its maximum value Δ_{max} at a wave-vector q_{max} which corresponds to the fastest growing mode (see Fig. 4).

Discussion – The growth rates of the pairing instability $\Delta_{q=0}^{\text{BCS}}$ and the ferromagnetic instabilities in the various channels $\Delta_{\text{max}}^{\text{FM}}$ are compared across the Feshbach resonance in Fig. 1. We have also included the naive RPA estimate of the growth rate of the Stoner instability in which we have replaced the Cooperon by $4\pi a/m$. From the comparison, we see that (1) the Cooperon suppresses the growth rate of the ferromagnetic instability but does not eliminate it, (2) the pairing and ferromagnetic instabilities compete over a wide range of interaction strength on both sides of the resonance, and (3) the pairing instability is always dominant. Our results suggest that even if there is a metastable ferromagnetic state [15], it probably cannot be reached via dynamic tuning of the interaction starting from a balanced gas. However, for short timescales $\sim (\Delta_{\text{max}}^{\text{FM}})^{-1} \sim (\Delta_{q=0}^{\text{BCS}})^{-1}$, both pairing and magnetic correlations will develop and may be detectable experimentally.

Comparison with experiment – The maximum of the pairing instability in the vicinity of $k_F a \approx 2$ closely matches the location of the transition found experimentally [11]. To inves-

tigate further, we plot the pairing rate as a function of interaction strength for several different temperatures in Fig. 2b. The shape of the pairing rate curve, especially at higher temperatures looks qualitatively similar to the atom loss rate (into pairs) found experimentally.

A fast rampdown of the magnetic field was used to convert weakly bound molecules into strongly bound molecules, and the kinetic energy of the remaining atoms was measured. It was found to have a minimum at $k_F a \approx 2$ [11]. We show that this minimum can be qualitatively understood within our analysis of the pairing instability. The energy of each molecule produced is given by $\sim \text{Re}[\omega_q]$ (see Fig. 2a). The molecular energy corresponds to the kinetic energy of the Fermions removed from the Fermi sea, measured with respect to the Fermi energy. Thus the rate of kinetic energy change of “unpaired” atoms is $\sim (\text{Re}[\omega_q] - 2\epsilon_F) \times \text{Im}[\omega_{q=0}]$ (see Fig. 2c). We find that the kinetic energy minimum is in the vicinity of the maximum of the pairing rate, in qualitative agreement with Ref. [11].

Acknowledgements – It is our pleasure to thank E. Altman, A. Chubukov, D. Huse, M. Lukin, S. Stringari, I. Carusotto, A. Georges and especially W. Ketterle for useful discussions. The authors acknowledge support from a grant from the Army Research Office with funding from the DARPA OLE program, CUA, the Swiss national Science Foundation, NSF Grant No. DMR-07-05472 NSF and PHY-06-53514, AFOSR-MURI, and the Alfred P. Sloan Foundation.

-
- [1] E. Stoner, *Phil. Mag.* **15**, 1018 (1933).
 - [2] J. Kanamori, *Prog. Theor. Phys.* **30**, 275 (1963).
 - [3] A. Tanaka, H. Tasaki, *Phys. Rev. Lett.* **98**, 116402 (2007).
 - [4] L. Chen, C. Bourbonnais, T. Li, and A.-M. S. Tremblay, *Phys. Rev. Lett.* **66**, 369 (1991).
 - [5] M. Houbiers, et al., *Phys. Rev. A* **56**, 4864 (1997); Y. Zhang and S. Das Sarma, *Phys. Rev. B* **72**, 115317 (2005); R. A. Duine and A. H. MacDonald, *Phys. Rev. Lett.* **95**, 230403 (2005); G. J. Conduit and B. D. Simons, *Phys. Rev. A* **79**, 053606 (2009); G. J. Conduit, A. G. Green, and B. D. Simons, *Phys. Rev. Lett.* **103**, 207201 (2009); G. J. Conduit and B. D. Simons, *Phys. Rev. Lett.* **103**, 200403 (2009).
 - [6] I. Bloch, J. Dalibard and W. Zwerger, *Rev. Mod. Phys.* **80**, 885 (2008).
 - [7] H. J. Miesner *et al.*, *Phys. Rev. Lett.* **82**, 2228 (1999); H. Schmaljohann, *Phys. Rev. Lett.* **92**, 040402 (2004); L. E. Sadler *et al.*, *Nature* **443**, 312 (2006).
 - [8] J. L. Roberts, N. R. Claussen, S. L. Cornish, E. A. Donley, E. A. Cornell, and C. E. Wieman, *Phys. Rev. Lett.* **86**, 4211 (2001).
 - [9] M. Greiner, O. Mandel, T.W. Hänsch, I. Bloch, *Nature* **419**, 51 (2002).
 - [10] N. Strohmaier *et al.*, *Phys. Rev. Lett.* **104**, 080401 (2010).
 - [11] G.-B. Jo *et al.*, *Science* **325**, 1521 (2009).
 - [12] L. J. LeBlanc, J. H. Thywissen, A. A. Burkov, and A. Paramekanti, *Phys. Rev. A* **80**, 013607 (2009).
 - [13] M. Babadi, D. Pekker, R. Sensarma, A. Georges, and E. Demler, arXiv:0908.3483.
 - [14] W. Ketterle and M. W. Zwiernlein, in *Proceedings of the International School of Physics “Enrico Fermi”, Course CLXIV*,

- Varenna, 20-30 June 2006, edited by M. Inguscio, W. Ketterle, and C. Salomon (IOS Press, Amsterdam, 2008).
- [15] S. Pilati, G. Bertaina, S. Giorgini, and M. Troyer, arXiv:1004.1169; S.-Y. Chang, M. Randeria, N. Trivedi, arXiv:1004.2680.
 - [16] A. Lamacraft and F. M. Marchetti, Phys. Rev. B **77**, 014511 (2008).
 - [17] N. V. Prokof'ev and B. V. Svistunov, Phys. Rev. B **77**, 125101 (2008).
 - [18] A. A. Abrikosov, L. P. Gorkov, I. E. Dzyaloshinski, *Methods of quantum field theory in statistical physics*, (Dover Publications, New York, 1975).
 - [19] H. V. Lohneysen, A. Rosch, M. Vojta and P. Wolfle, Rev. Mod. Phys. **79**, 1015 (2007).